ONE-STEP ELECTROGENERATED MANGANESE OXIDE/CARBON COMPOSITE AS POTENTIAL ELECTRODE MATERIAL FOR PSEUDO-SUPERCAPACITORS

N. Giorgadze[1], L. Londaridze[2], L. Kvinikadze[1,3], F. Lisdat[4], N. Nioradze[1*]

[1]R. Agladze Institute of Inorganic Chemistry and Electrochemistry, Ivane Javakhishvili Tbilisi State University, 11 Mindeli Str., Tbilisi 0186, Georgia
[2]Faculty of Exact and Natural Sciences, Ivane Javakhishvili Tbilisi State University, Tbilisi, Georgia
[3]Faculty of Pharmacy, Tbilisi State Medical University, Tbilisi, Georgia
[4]Biosystems Technology, Institute of Life Sciences and Biomedical Technologies, Technical University of Applied Sciences Wildau, Wildau, Germany
[*]e-mail: nikoloz.nioradze@tsu.ge

Received 03.07.2025
Accepted 21.10.2025

Abstract: *The increasing demand for energy worldwide has led to the development of supercapacitors, which are energy storage devices known for their high-power density, quick charging and discharging capabilities, large capacity, long lifespan, and environmental benefits. Here, we discuss the method for synthesizing manganese oxide/carbon composite materials through a one-step electrolysis process for potential application as supercapacitive electrode materials. The deposition of manganese oxide on graphite, together with the exfoliation of carbon flakes from the graphite electrodes induced by gas evolution during water electrolysis, led to the electrogeneration of a manganese oxide–carbon composite powder. After investigation of physical properties, the powder of manganese oxides/carbon composite was coated onto planar indium tin oxide (ITO) electrodes. Evaluation of the electrochemical performance and charge storage capacity revealed that ITO electrodes modified with the electrogenerated composite exhibited superior electrochemical performance compared with those modified only with a physical mixture of manganese oxide and carbon nanotubes.*
Keywords: *Chronoamperometry, electrosynthesis, specific capacitance*

1. Introduction

Experiencing the diminishing supply of fossil fuels and increasing signals of climate change, sustainable and renewable energy technologies are being increasingly progressed (such as solar, hydro, wind, and tidal energy), and intensive growth of renewable energy production is happening. Since renewable energy sources such as solar and wind typically exhibit on-peak and off-peak fluctuations, electrochemical energy storage systems—including rechargeable batteries and electrochemical capacitors (ECs), or supercapacitors—are attracting increasing attention [1–4].

Bridging the gap between conventional capacitors and batteries, supercapacitors are characterized by a combination of high power density and sufficient energy density, which can be a suitable solution to emerging energy applications. The energy stored in ECs can be either capacitive (non-Faradaic) or pseudocapacitive (Faradaic). The former involves charge separation at the electrode/electrolyte interface, while the latter relies on redox reactions at the electrode materials [5, 6]. The use of supercapacitors in classical applications has led to significant improvements in specific parameters over the last decade, with researchers achieving notable progress in areas such as biofuel cells. Several attractive systems have been constructed as a result [7-10]. Furthermore, it has been demonstrated that supercapacitors have the potential to further enhance their performance [11, 12].

Among widely used active electrode materials for energy conversion systems and specifically for supercapacitors, such as carbon, transition metal oxides, and conducting polymers, manganese oxides have gained attention as electrocatalytic and electrode materials for hydrogen generation and energy conversion systems such as supercapacitors (SCs) due to their high specific capacitance, abundance, low cost, and eco-friendly nature [13-16]. Manganese can exist in various oxidation states, resulting in the formation of a range of stable oxides (MnO, Mn_3O_4, Mn_2O_3, MnO_2). These oxides possess diverse crystal structures, defect chemistry, morphology, and textures, which significantly influence their electrochemical properties. As a result, manganese oxides are widely

used as electrode materials in energy conversion and storage devices, including batteries and supercapacitors [17 - 21].

To achieve optimal electrochemical performance, electrode materials for batteries and supercapacitors must possess good conductivity. When the solid-state diffusion rate of electrons is hindered by poor conductivity, the power density and energy density of the battery or supercapacitor can decrease significantly. Hence, the low electrical conductivity of manganese oxides is a significant drawback, leading to extensive research on enhancing their conductive capabilities. Electrical conductivity can be increased by forming composite materials using highly conductive materials such as carbon or graphene. In addition, nanorods, nanospheres, and mesoporous structures have all shown significant improvements in the specific capacitance of manganese oxide-based electrodes [22-24].

This paper presents a one-step simultaneous electrosynthesis of manganese oxide/carbon composites for use as potential electrode materials in energy storage devices. The electrodes were prepared by depositing a mixture of manganese oxides and carbon powder onto indium-tin oxide glass slides. The morphological and electrochemical properties of the composite were then studied.

2. Experimental part

2.1 Materials and chemicals. Manganese sulphate monohydrate was purchased from Sigma Aldrich (ACS reagent >98%) to prepare an aqueous solution for the electrosynthesis of manganese oxide/carbon powder. Manganese (IV) oxide (Sigma-Aldrich, >99.0%) was used to prepare a mixture with carbon nanotubes (multi-walled carbon nanotube powder, Graphene Supermarket, USA). Sodium sulphate was used for electrolyte preparation (Sigma-Aldrich, >99.0%). Polyethylene oxide (PEO) was used to prepare a coating mixture (Sigma-Aldrich, average Mv 600 000). Ethanol (Sigma-Aldrich, 96%) mixed with water was used as a solvent for the preparation of a suspension of manganese oxide/carbon/PEO. DI water with a resistivity of 18.2 MΩ·cm was used to prepare all aqueous solutions.

Indium-tin oxide-coated glass (Sigma Aldrich, surface resistivity 15-25 Ω/sq) served as the substrate for the electrode. Graphite plates (Sigma Aldrich, SymLectro Graphite Electrodes; dimensions: 3 x 20 x 60 mm) were used as working and counter electrodes. Ag/AgCl was used as a reference electrode (CH Instrument, TX, USA).

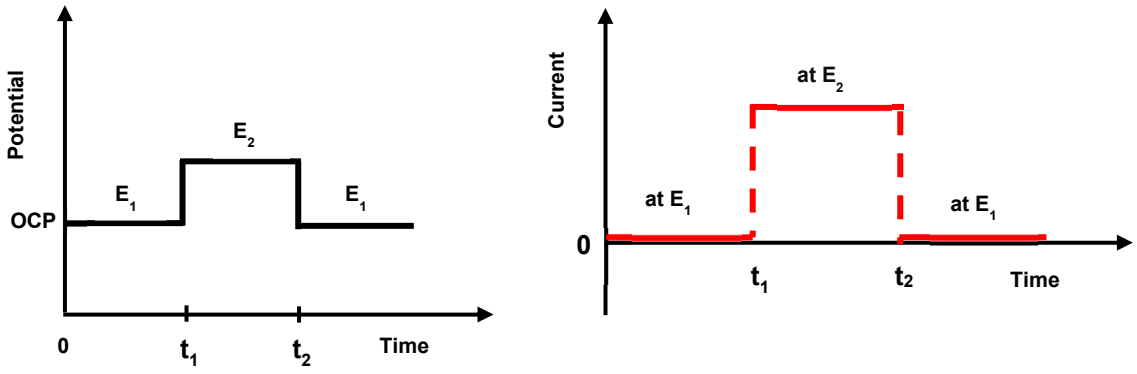

Fig. 1. Profile of the applied potential change for the chronoamperometric measurement (left) and schematic illustration of the resulting current profile (right)

2.2 Preparation of manganese oxide/carbon powder mixture. Manganese oxide/carbon powder composite was prepared by the electrolysis in manganese sulphate/sodium sulphate aqueous electrolyte (0.5 M $MnSO_4$ and 0.4 M Na_2SO_4). Chronoamperometry was applied to the three-electrode system consisting of a graphite working and counter electrode and a silver/silver chloride reference electrode. First, an open circuit potential (OCP) of the system was measured, and then chronoamperometry was performed, changing the potential of a working electrode between OCP and

an extreme positive potential value (4.0 V vs Ag/AgCl). The time gap between the two alternating potentials was 10 seconds, with each potential being applied for 10 seconds. Fig. 1 provides a schematic illustration of the applied potentials and the resulting current profile. During the process of electrolysis, manganese oxide forms on the graphite working electrode, while the carbon material (graphite working electrode) simultaneously deteriorates, resulting in the formation of deposits at the bottom of the electrochemical cell. The resulting powder consisting of manganese oxide/carbon flakes was then dried at room temperature.

2.3 Preparation of ITO substrate working electrode. ITO-coated glass chip electrodes were modified using a spin-coating method (spin coater Ossila, UK), depositing the mixture of manganese oxide/carbon powder (Mn_xO_y/C) onto the pre-cut and pre-cleaned (in acetone, ethanol, and isopropanol for 15 minutes in each) ITO surface to prepare the working electrodes for electrochemical testing. MnxOy/C/PEO mixture was prepared by adding 4 wt.% of PEO and 0.5 wt.% of MnxOy/C (thoroughly premixed using Vortex) in small portions to a solution of EtOH/H_2O (ratio 1.5/1) while stirring. The mixture was continuously stirred for 2 hours. For spin-coating, a pre-cleaned ITO chip was placed on a spinning disk, with only a portion (5.0 mm x 5.0 mm) of the area exposed, and the rest covered with parafilm. Each droplet (6 droplets, totalling approximately 0.2 g) of the mixture was then dropped onto the exposed area of the stationary ITO glass chip and spun at 2000 rpm for 20 seconds. After spin-coating, the composite was sintered on a heating plate under air at 500 °C and cooled down gradually.

2.4 Electrochemical and physical characterization of manganese/carbon powder. Electrochemical measurements, such as open circuit potential detection, cyclic voltammetry (CV), and galvanostatic charge-discharge measurements, were performed using CH Instrument (CH Instrument 1140c, Austin, TX, USA). Electrochemical impedance spectroscopy (EIS) was performed in the range of 10 kHz to10 mHz with an amplitude of 5 mV by CH 660F. We used a homemade electrochemical cell with a volume of 30 mL, arranging all three electrodes from the cover down into the solution. X-ray diffraction measurements were taken on ДРОН-4.07 (Burevestnik, Russia) with $Cu_{k\alpha}$ (λ=1.54184 Å) radiation (X-ray tube voltage – 40 kV; current – 20 mA). Scanning electron microscopy and energy dispersive spectroscopy were conducted on a JSM-6510 series JEOL Ltd. (Japan). Thermogravimetric analysis was performed using the instrument TG 209 F3 (NETZSCH, Germany). To analyse the amount of manganese on ITO, the surface of the ITO electrode was dissolved in 0.2 M oxalic acid for 7 days and analysed using atomic adsorption spectroscopy (PerkinElmer Analyst 200 Atomic Absorption Spectrometer).

3. Results and Discussion

Manganese oxides can be prepared using various methods, including hydrothermal [25], precipitation [26], sol-gel [27], electrodeposition [28, 29], and others [30, 31]. However, these oxides are typically produced as powders and cannot be directly used as electrodes. Instead, they must be mixed with conductive materials and binders with specific ratios [32, 33]. Our approach involves combining electrochemistry and spin-coating to create a composite of manganese oxide and carbon, ensuring intimate contact between the two components. This mixture is then applied to planar electrode chips to create working electrodes.

The composite of manganese oxides and carbon flakes was prepared in one step using chronoamperometry in a three-electrode system with graphite plates as working electrodes. A similar procedure has been reported for synthesis of Fe_2O_3/graphene by Wenyu Zhang et al [34]. During chronoamperometry, the high potential was +4.0V versus Ag/AgCl, while the open circuit potential was applied as a low potential. Every 10 seconds the potential was switched from high to low and vice versa. The procedure resulted in two simultaneous processes: 1) the deposition of manganese oxide on the carbon working electrode, and 2) the disassembly of the carbenous working electrode resulting in the deposition of the composite particles on the cell bottom and in solution. The filtered and washed composite showed a close contact between the two components (Mn_xO_y and carbon).

Fig. 2 illustrates the current-time profiles that have typically been obtained during the electrosynthesis process. The graph illustrates that only the time periods of high potential are responsible for the preparation. Here, not only the oxidation of Mn^{2+} ions, but also the oxidation of water occurs with gas bubble development. The latter can be considered as the main reason for the observed disassembly of the carbon material of the working electrode. After the potential is switched back to OCP, the current stabilizes rather quickly at zero values. However, transient cathodic currents indicating back reaction are also clearly visible.

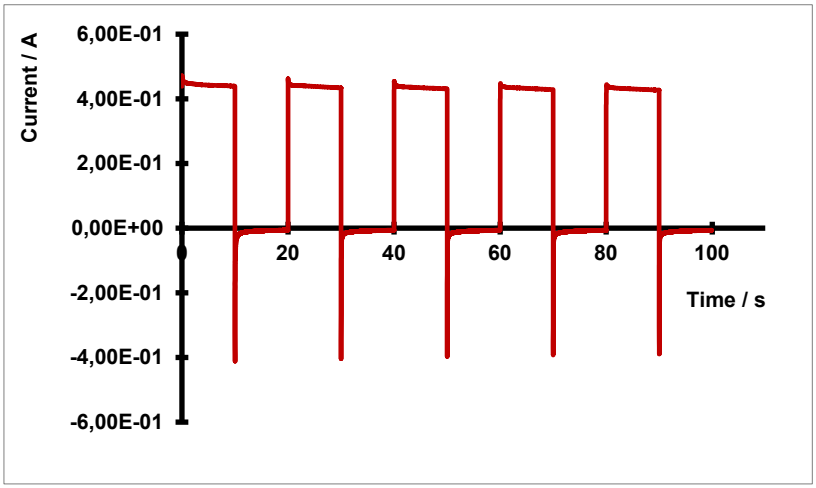

Fig. 2. Current-time profiles obtained during the chronoamperometric formation of the MnxOy/C composite. Electrolyte: 0.5 M $MnSO_4$ / 0.4 M Na_2SO_4. Graphite working and counter electrodes. The potential was changed from 0.025 V (OCP) to 4.0 V vs Ag/AgCl

The electrochemical oxidation of Mn^{2+} ions can be explained based on the redox chemistry of manganese, as follows [35]:

$$Mn^{2+} \rightarrow Mn^{3+} + e \quad (1)$$
$$Mn^{3+} + H_2O \rightarrow MnOOH + H^+ \quad (2)$$
$$MnOOH \rightarrow MnO_2 + H^+ + e \quad (3)$$

As an alternative route of Mn(III) disproportionation can also occur:

$$2Mn^{3+} \rightarrow Mn^{2+} + Mn^{4+} \quad (4)$$
$$Mn^{4+} + 2H_2O \rightarrow MnO_2 + 4H^+ \quad (5)$$

In any of the paths [35] MnO_2 is formed on the graphite electrode. The vigorous generation of gases due to electrolysis of water contributes to exfoliation of the graphite electrode. The evolved oxygen most likely penetrates into the interstitial space between graphite layers and forces the material to the point of splitting into flakes, like a few-layered graphene [36]. The presence of highly hydrated sulphate ions may also contribute to this process. In situ prepared MnO_2 can mainly precipitate on graphite before exfoliation and be detached from the electrode together with graphene flakes. In addition, it can be deposited on exfoliated graphite particles, as long as they are in electrical contact with the main electrode body.

The combined process of manganese oxidation and graphite exfoliation has been chosen in order to achieve both - a close contact of the two materials and a high surface area. The latter is rather important for the capacitive properties of the obtained composite, when applied as electrode material. Consequently, liquid nitrogen cryosorption was performed on the Mn_xO_y/graphene composites to determine the surface area and porosity. Structural parameters of the powder, such as the specific surface area (Brunauer-Emmett-Teller surface area, S_{BET}) and adsorption average pore diameter (4V/A by BET) were found to be 39.54 m^2/g and 1.39 nm, respectively. Thus, the product of the

electrosynthesis shows only a moderate specific surface area. Despite these rather low numbers, the results still might be promising, since some crystallized compounds (unlike amorphous MnO_2) do not show strict dependence of the capacitance on the BET surface area. In some cases, crystalline compounds with relatively low surface area (lower than 100 m^2/g) showed capacitance values exceeding 200 F/g [37].

For the analysis of the thermal behaviour of the obtained composite, thermogravimetric analysis was performed. Thermal measurements for the samples were carried out using TGA and DTA. In order to elucidate the special features of the prepared Mn_xO_y/C as a composite, simple mixtures of manganese oxide powder and carbon nanotubes have been prepared and analysed. Fig. 3 shows TGA and DTA spectra of a mixed powder of manganese oxide and carbon and an electrogenerated composite of both materials.

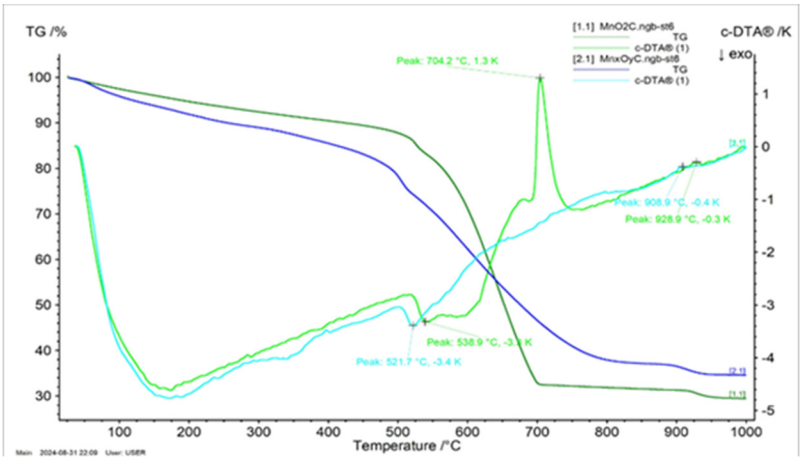

Fig. 3. TGA and DTA thermograms of manganese oxide/carbon powder. Dark and light blue curves represent TGA and DTA analysis for electrogenerated manganese oxides-carbon composite. Dark and light green curves represent TGA and DTA for the manganese (IV) oxide – carbon nanotube mixture, respectively

The pathway of the thermal behaviour exhibited by thermographs for both mixtures demonstrates similar characteristic profiles, but with some differences due to the specificity of used materials. The weight loss of the Mn_xO_y/C composite (blue line) can be divided into several main stages (TGA plots) with approximately 30% of the total weight. The first segment until 500 °C is due to the removal of physically adsorbed surface water and structural water and to the desorption of surface-active oxygen. DTA analysis (light blue line) shows the endothermic peaks at around 170 °C which could be related to the dehydration process. The next range (around 500 °C) indicates evolution (a small endothermic peak at around 550 °C) of lattice oxygen and phase transformation from MnO_2 to Mn_2O_3 and then Mn_3O_4 at around 900 °C [38]. The steep change of the thermogram starting at about 570 °C should be related to the burning of carbon nanoflakes, which resulted in a mass drop to almost 30 %. A very similar trend is shown by the commercial MnO_2 and carbon nanotube mixture (green and light green lines for TGA and DTA, respectively), except that for the TGA curve, a steeper change of mass happens at about 570 °C indicating faster burning of carbon nanotubes compared to indirectly electrogenerated (exfoliated) carbon flakes. The additional peak on the DTA curve at the temperature of 705 °C shows the maximum oxidation rate of particles not well bound to manganese oxide. This value that is close to the reported one [39] confirms the different coexistence of manganese oxide and carbon nanostructure compared to electrogenerated manganese oxide and exfoliated carbon nanoparticles.

Phase composition and crystallographic structure of the obtained composite (electrogenerated manganese oxide-carbon) have been analysed after transferring the material onto an ITO glass slide and calcining at 500 °C for one hour in the presence of air. Note that a polymer (PEO) was also introduced during deposition of the composite material by applying a fairly simple centrifugation

procedure (which, however, will degrade during the subsequent heating step). The X-ray diffraction patterns of the calcined composite surface are shown in Fig. 4.

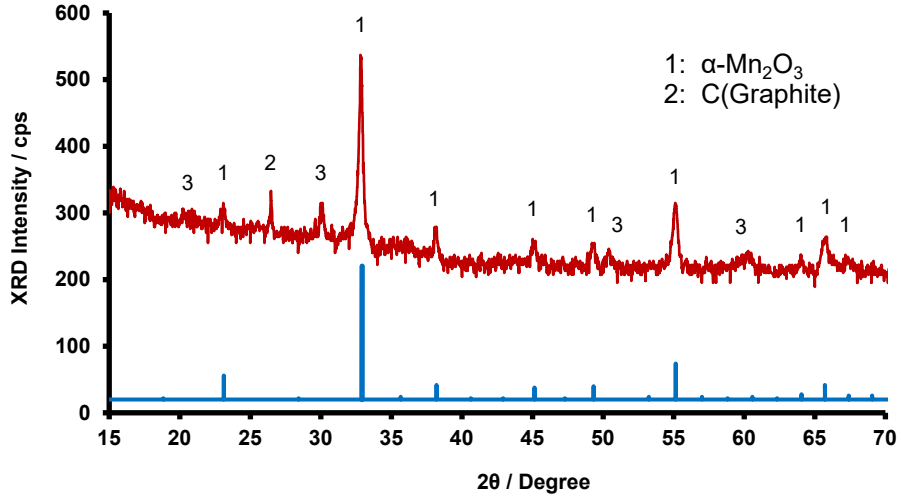

Fig. 4. XRD patterns of the calcined composite of Mn_xO_y/carbon powder

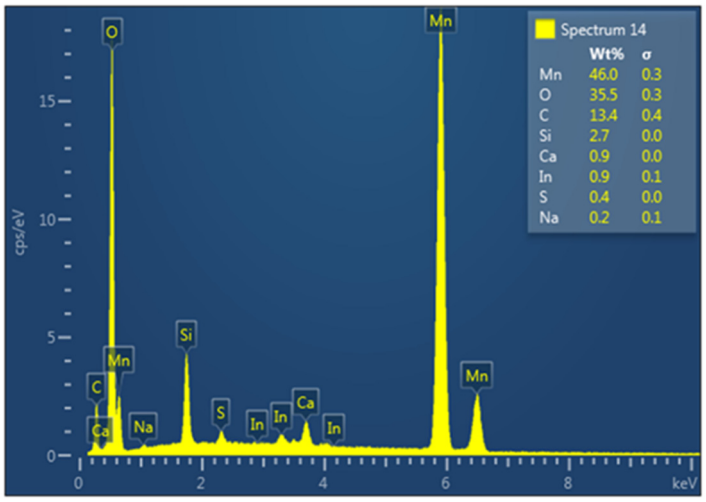

a)

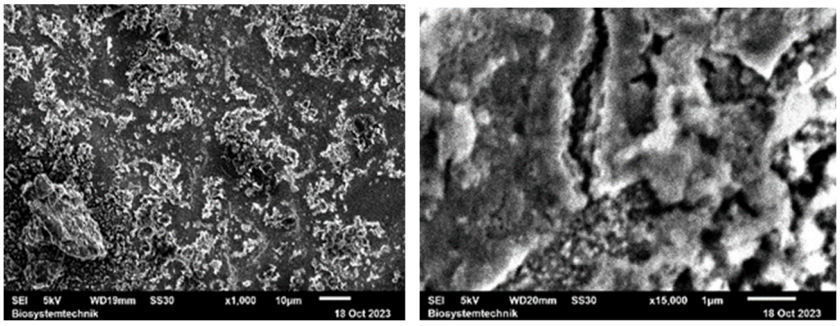

b) c)

Fig. 5. Characterisation of the prepared Mn_xO_y/C composite: a) EDX image showing the presence of Mn, carbon, and oxygen along with Si and In coming from the ITO glass, Na probably incorporated from the solution, and Ca from an unidentified source. The inset shows the percent composition of the electrode surface (b, c) SEM investigation of the surface of the composite electrode. White bars in b) and c) represent a length of 10 and 1 µm, respectively

The diffractogram of the Mn_xO_y/C-ITO sample mainly contains phase maxima related to α-Mn_2O_3 (Fig. 4, red line). Comparatively low intensities are observed for relative diffraction maxima

of carbon and ITO. No other crystalline phases were detected in the diffraction pattern, which confirms the high purity of the composition. The blue line represents a pure α-Mn_2O_3 (National Bureau of Standards). The good crystalline nature of the prepared samples is manifested by the sharp XRD peaks, which could lead to improving the electron transport efficiency at the electrode/electrolyte interface. The peaks appearing at 2θ = 23.19°, 32.84°, 38.15°, 45.17°, 49.40°, 55.18°, 64.04°, and 65.81° can be attributed to the (211), (222), (400), (332), (431), (440), and (622) planes of α-Mn_2O_3 [24].

Energy dispersive spectroscopy proved the presence of manganese on the surface of composite electrodes (Fig. 5, a). It also revealed the presence of other components, such as oxygen and carbon, which could result from the exfoliation of graphite and the remaining carbon after calcination of PEO. Sodium on the spectrogram appeared because of its incorporation from the electrolyte solution. SEM images (Fig. 5 b, c) verify the coverage of the ITO surface with the manganese oxide/carbon composite by means of the selected spin-coating procedure. The structures of undefined shape with micro canyons and valleys appear over the whole surface.

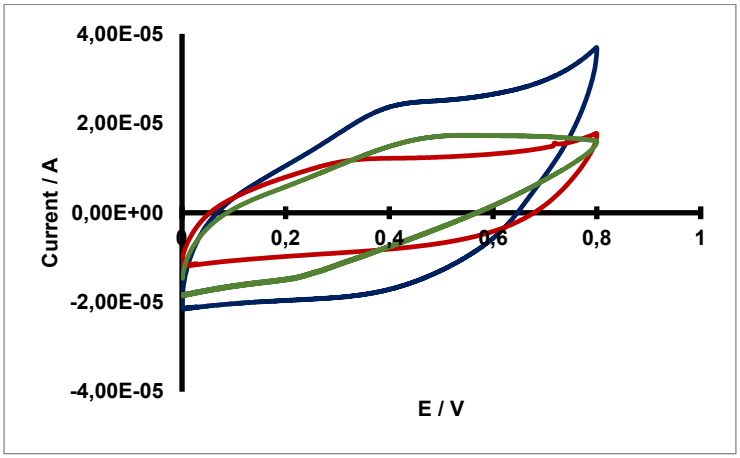

Fig.6. Cyclic voltammetry of composite (Mn_xO_y/C) and mixed (MnO_2/carbon nanotubes) electrodes deposited on ITO glass: *blue curve* – electrogenerated composite, *red curve* – 9 to 1 mixture (MnO_2/carbon nanotube), green – 5 to 5 mixture (MnO_2/carbon nanotube). Solution: 0.1 M Na_2SO_4; scan rate - 0.1 V/s

Finally, the electrochemical characteristics of the electrogenerated manganese oxide-carbon composite have been studied. For comparison, the simple mixture of manganese oxide and carbon nanotubes (9/1 and 5/5 ratios) has been analysed again. For this purpose, both materials have been applied on ITO electrodes and calcined after a spin-coating method of deposition. Here the same overall amount has been used. Fig. 6 demonstrates differences between the cyclic voltammograms of electrodes modified in one case (blue curve) by electrogenerated manganese oxide-carbon composite and in another case (red and green curves) by mechanically mixed manganese (IV) oxide and carbon nanotubes in sodium sulfate solution. The ratio of the mechanically mixed commercial manganese (IV) oxide and carbon nanotubes is taken as 9/1 (red curve) and 5/5 (green curve).

The voltammetry of electrogenerated composite showed high capacitive currents in comparison to the simple mixtures of manganese oxide and carbon nanotubes. The higher performance characteristics of the electrogenerated composite are probably associated with better contact between manganese oxide and carbon flakes - as the particles of a connecting component formed due to the exfoliation of carbon layers of graphite electrodes together with manganese oxides deposited on them.

In order to evaluate the charge storage capacities of the prepared Mn_xO_y/C composite on ITO, galvanostatic charge/discharge (GCD) measurements have been conducted. The results presented in Fig. 7 show that the GCD curves are not very symmetrical but have a typical triangular shape at different charging currents, indicating that the composite electrodes have certain charge/discharge properties. In addition, we can conclude about the reversible behaviour.

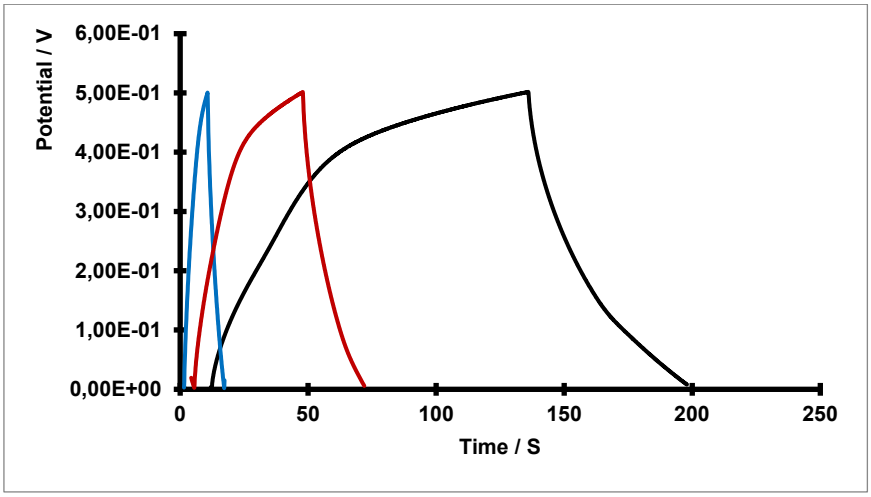

Fig. 7. Galvanostatic charge/discharge (GCD) curves at different current densities within the same voltage window of 0-0.5 V taken on electrogenerated manganese oxide-carbon (Mn_xO_y/C) composite modified electrode. Solution: 0.1 M Na_2SO_4. Charge-discharge currents: 5 x 10^{-6} A (blue), 2 x 10^{-6} A (red), 1 x 10^{-6} A (black)

The specific capacitance values can be calculated using the following equation:

$$C = \frac{I \times \Delta t}{m \times \Delta V} \qquad (1)$$

where I is the applied constant current (A), m is the mass of active material (Mn_xO_y only, g), ΔV is the potential window during cycling, and Δt is the time of cycle (s). The mass of the manganese oxide within the composite has been obtained as follows: The composite electrode was immersed in 0.2 M oxalic acid, and subsequently the solution was analyzed for the manganese content, which allowed the determination of specific capacitance with a value of 95.8 F/g. The former is similar to the one obtained from the analysis of the charging behaviour by cyclic voltammetry (131 F/g at 0.1 V/s scan rate).

Results for electrochemical impedance spectroscopy are depicted in Fig. 8.

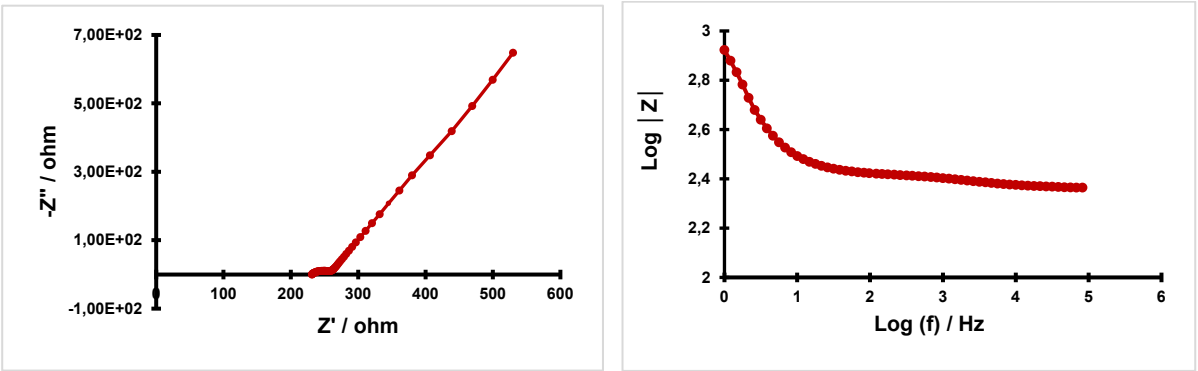

a) b)

Fig. 8. Electrochemical impedance spectra: Nyquist plot (a) and Bode plot (b) of the studied electrode

The representative Nyquist plot (a) of the sample in Fig. 8 shows a steep line with the angle higher than 45 degrees to the real axis at the low-frequency region and a small depressed semicircle in the high-frequency region exhibiting capacitive characters of the sample [40]. The slope line portion of the curve is a representation of frequency-dependent ion diffusion in the electrolyte to the electrode surface. The slope value is related to the speed of electric double layer formation.

Different capacitance values can be found in literature for such types of materials. The obtained capacitances are not extremely high, but they may serve as a good starting point for further enhancement by change in parameters during the preparation [17, 22, 37].

4. Conclusions

In this study, manganese oxide/carbon composites were synthesized by one-step electrolysis in an aqueous solution of manganese and sodium sulfates. The electrochemical exfoliation of graphite electrodes along with electrochemical oxidation of manganese was observed during the process. The obtained composite can easily be separated from the electrolyte solution to apply as the electrode material on planar ITO electrode by the spin-coating procedure. The composite material was analyzed to determine material properties and the electrochemical parameters. From the cyclic voltammetry it can be concluded that the charge storage properties are improved, which was further confirmed by galvanostatic charge-discharge measurements. Moderate values of specific capacitance have been found, which represent the basis for further optimization. Electrode preparation can also be seen as a tool to improve porosity and conductivity, along with the electrical generation of the material itself.

Acknowledgment. This work was supported by Shota Rustaveli National Science Foundation of Georgia, (Grant number: FR-22-11993).

References

1. Conway B.E. *Electrochemical supercapacitors: scientific fundamentals and technological applications*. New York. Plenum Press. 1999. 607 p.
2. Yang Z., Zhang J., Kintner-Meyer M. C., Lu X., Choi D., Lemmon J. P., and Liu J. Electrochemical energy storage for green grid. *Chem. Rev*. 2011, **Vol. 111**, p. 3577–3613. DOI: 10.1021/cr100290v
3. Palchoudhury S., Ramasamy K., Gupta R.K., Gupta A. Flexible supercapacitors: a materials perspective. *Front. Mater.* 2019, **Vol. 5(83)**, 83. DOI: 10.3389/fmats.2018.00083
4. Xiong C., Wang T., Zhao Z., Ni Y. Recent progress in the development of smart supercapacitors, *SmartMat*. 2023, **Vol. 4,** e1158. DOI: 10.1002/smm2.1158
5. Forse A.C., Merlet C., Griffin J.M., Grey C.P. New Perspectives on the Charging Mechanisms of Supercapacitors. *J. Am. Chem. Soc.* 2016, **Vol. 138,** p. 5731−5744. DOI:10.1021/jacs.6b02115
6. Kumar N., Kim S.-B., Lee S.-Y., Park S.-J. Recent Advanced Supercapacitor: A Review of Storage Mechanisms, Electrode Materials, Modification, and Perspectives. *Nanomaterials*. 2022, **Vol. 12**, 3708. DOI:10.3390/nano12203708
7. Cosnier S., Gross A.J., Le Goff A., Holzinger M. Recent advances on enzymatic glucose/oxygen and hydrogen/oxygen biofuel cells: Achievements and limitations. *Journal of Power Sources*, 2016, **Vol. 325**, p. 252-263. DOI:10.1016/j.jpowsour.2016.05.133
8. Bollella P., Fusco G., Stevar D., Gorton L., Ludwig R., Ma S., Boer H., Koivula A., Tortolini C., Favero G., Antiochia R., Mazzei F. A Glucose/Oxygen Enzymatic Fuel Cell based on Gold Nanoparticlesmodified Graphene Screen-Printed Electrode. Proof-of-Concept in Human Saliva. *Sensors and Actuators B: Chemical.* 2017, **Vol. 256**, p. 921-930. DOI:10.1016/j.snb.2017.10.025
9. Göbel G., Beltran M.L., Mundhenk J., Heinlein T., Jörg Schneider, Lisdat F. Operation of a carbon nanotube-based glucose/oxygen biofuel cell in human body liquids—Performance factors and characteristics. *Electrochimica Acta.* 2016, **Vol. 218**, p. 278-284. DOI:10.1016/j.electacta.2016.09.128
10. Scherbahn V., Putze M.T., Dietzel B., Heinlein T., Schneider J.J., Lisdat F. Biofuel cells based on direct enzymeelectrode contacts using PQQ-dependent glucose dehydrogenase / bilirubin oxidase and modified carbon nanotube materials. *Biosensors and Bioelectronics*, 2014, **Vol. 61**, p. 631-638. DOI:10.1016/j.bios.2014.05.027

11. Pankratov D., Conzuelo F., Pinyou P., Alsaoub S., Schuhmann W., Shleev S. A Nernstian Biosupercapacitor. *Angew. Chem. Int. Ed.* 2016, **Vol. 55**, p. 15434 –15438. DOI: 10.1002/anie.201607144
12. Agnès C., Holzinger M., Le Goff A., Reuillard B., Elouarzaki K., Tingry S., Cosnier S. Supercapacitor/biofuel cell hybrids based on wired enzymes on carbon nanotube matrices: Autonomous reloading after high power pulses in neutral buffered glucose solutions. *Energy Environ. Sci.* 2014, **Vol. 7**, p. 1884-1888. DOI:10.1039/C3EE43986K.
13. Tadesse M.G., Ahmmed A.S., Lübben J.F. Review on Conductive Polymer Composites for Supercapacitor Applications. *J. Compos. Sci.* 2024, **Vol. 8**, p. 53. DOI:10.3390/jcs8020053
14. Zhai Z., Zhang L., Duc T., Ren B., Xu Y., Wanga S., Miao J., Liu, Z. A review of carbon materials for supercapacitors. *Materials & Design*. 2022, **Vol. 221**, 111017. DOI:10.1016/j.matdes.2022.111017
15. Abdaha M.A.A.M., Azmana N.H.N., Kulandaivalua S., Sulaiman Y. Review of the use of transition-metal-oxide and conducting polymer-based fibres for high-performance supercapacitors. *Materials and Design.* 2020, **Vol. 186**, 108199. DOI: 10.1016/j.matdes.2019.108199
16. Aliyev A.Sh., Guseynova R.G., Gurbanova U.M., Babanly D.M., Fateev V.N., Pushkareva I.V., Tagiyev D.B. Electrocatalysts for Water Electrolysis. *Chemical Problems,* 2018, **Vol. 3(16)**, p. 283-306. DOI:10.32737/2221-8688-2018-3-283-306
17. Lee H.Y., Goodenough J.B. Supercapacitor Behaviour with KCl Electrolyte. *Journal of Solid State Chemistry*. 1998, **Vol. 144**, p. 220-223.
18. Wu D., Xie X., Zhang Y., Zhang D., Du W., Zhang X., Wang B. MnO_2/Carbon Composites for Supercapacitor: Synthesis and Electrochemical Performance. *Front. Mater*. 2020, **Vol. 7**, 2. DOI:10.3389/fmats.2020.00002
19. Nagamuthua S., Ryu K.-S. MOF-derived microstructural interconnected network porous Mn_2O_3/C as negative electrode material for asymmetric supercapacitor device. *CrystEngComm.* 2019, **Vol. 21**, p. 1442-1451. DOI: 10.1039/C8CE01683F
20. Sambandam B., Mathew V., Kim S., Lee S., Kim S., Hwang J.Y., Fan H.J., Kim J. An analysis of the electrochemical mechanism of manganese oxides in aqueous zinc batteries. *Chem.* 2022, **Vol. 8(4)**, p. 924–946. DOI: 10.1016/j.chempr.2022.03.019
21. Wei W., Cui X., Chena W., Ivey D.G. Manganese oxide-based materials as electrochemical supercapacitor electrodes. *Chem. Soc. Rev*. 2011, **Vol. 40**, p. 1697–1721. DOI: 10.1039/c0cs00127a
22. Kim M., Yoo M., Yoo Y., Kim J. Capacitance behavior of composites for supercapacitor applications prepared with different durations of graphene/nanoneedle MnO_2 reduction. *Microelectronics Reliability*. 2014, **Vol. 54**, p. 587–594. DOI: 10.1016/j.microrel.2013.11.005
23. Patel M.N., Wang X., Wilson B., Ferrer D.A., Dai S., Stevenson K.J., Johnston K.P. Hybrid MnO_2–disordered mesoporous carbon nanocomposites: synthesis and characterization as electrochemical pseudocapacitor electrodes. *J. Mater. Chem.* 2010, **Vol. 20**, p. 390–398. DOI: 10.1039/b915370e
24. Hou Y., Cheng Y., Hobson T., Liu J. Design and Synthesis of Hierarchical MnO_2 Nanospheres/Carbon Nanotubes/Conducting Polymer Ternary Composite for High Performance Electrochemical Electrodes. *Nano Lett*. 2010, **Vol. 10**, p. 2727–2733. DOI: 10.1021/nl101723g
25. Chandiran K., Murugesan R.A., Balaji R., Andrews N.G., Pitchaimuthu S., Raja K.C. Long single crystalline α-Mn_2O_3 nanorods: facile synthesis and photocatalytic application. *Mater. Res. Express*. 2020, **Vol. 7**, 074001. DOI: 10.1088/2053-1591/ab9fbd
26. Kurniati S., Asleni, Linggawati A., Siregar S.S., Awaluddin A. Synthesis and Catalytic Activities of Manganese Oxides Prepared by Precipitation Method: Effects of Mixing Modes of Reactants and Calcination Process. *Journal of Physics: Conference Series.* 2019, **Vol. 1351,** 012035. DOI: 10.1088/1742-6596/1351/1/012035

27. Wang X., Wang X., Huang W., Sebastian P.J., Gamboa S. Sol–gel template synthesis of highly ordered MnO_2 nanowire arrays. *Journal of Power Sources*. 2005, **Vol. 140,** p. 211–215. DOI:10.1016/j.jpowsour.2004.07.033
28. Sergienko N., Radjenovic J. Manganese oxide-based porous electrodes for rapid and selective (electro) catalytic removal and recovery of sulfide from wastewater. *Applied Catalysis B: Environmental.* 2020, **Vol. 267,** 118608. DOI:10.1016/j.apcatb.2020.118608
29. Lee C.Y., Tsai H.M., Chuang H.J., Li S.Y., Lin P., Tsenga T.Y. Characteristics and Electrochemical Performance of Supercapacitors with Manganese Oxide-Carbon Nanotube Nanocomposite Electrodes. *Journal of The Electrochemical Society*, 2005, **Vol. 4(152)**, p. A716-A720. DOI 10.1149/1.1870793
30. Zolfaghari A., Ataherian F., Ghaemi M., Gholami A. Capacitive behavior of nanostructured MnO_2 prepared by sonochemistry method. *Electrochimica Acta.* 2007, **Vol. 52**, p. 2806–2814. DOI:10.1016/j.electacta.2006.10.035
31. Ghaemia M., Ataherian F., Zolfaghari A., Jafari S.M. Charge storage mechanism of sonochemically prepared MnO_2 as supercapacitor electrode: Effects of physisorbed water and proton conduction. *Electrochimica Acta*. 2008, **Vol. 53**, p. 4607–4614. DOI:10.1016/j.electacta.2007.12.040
32. Hu Z., Zu L., Jiang Y., Lian H., Liu Y., Li Z., Chen F., Wang X., Cui X. High Specific Capacitance of Polyaniline/Mesoporous Manganese Dioxide Composite Using KI-H_2SO_4 Electrolyte. *Polymers.* 2015, **Vol. 7,** p. 1939–1953. DOI:10.3390/polym7101491
33. Jadhav S.A., Dhas S.D., Patil K.T., Moholkar A.V., Patil P.S. Polyaniline (PANI)-manganese dioxide (MnO_2) nanocomposites as efficient electrode materials for supercapacitors. *Chemical Physics Letters.* 2021, **Vol.** 778, 138764. DOI:10.1016/j.cplett.2021.138764
34. Zhang W., Zeng Y., Xu C., Tan H., Liu W., Zhu J., Xiao N., Hoon Hng H., Ma J., Hoster H.E., Yazami R., Yan Q. Fe_2O_3 nanocluster-decorated graphene as O_2 electrode for high energy Li–O_2 batteries. *RSC Advances*. 2012, **Vol. 22(2)**, p. 8508–8514. DOI: 10.1039/C2RA20757E
35. Huang W., Li J., Xu Y. Nucleation/growth mechanisms and morphological evolution of porous MnO_2 coating deposited on graphite for supercapacitor. *Materials.* 2017, **Vol. 10,** 1205. DOI:10.3390/ma10101205
36. Ilnicka A., Skorupska M., Kamedulski P., Lukaszewicz J.P. Electro-Exfoliation of graphite to graphene in an aqueous solution of inorganic salt and the stabilization of its sponge structure with Poly(Furfuryl Alcohol). *Nanomaterials.* 2019, **Vol. 9,** 971. DOI:10.3390/nano9070971
37. Brousse T., Toupin M., Dugas R., Athouël L., Crosnier O., Bélanger D. Compounds in Electrochemical Supercapacitors Crystalline MnO_2 as Possible Alternatives to Amorphous. *J. Electrochem. Soc.* 2006, **Vol. 153(12),** p. A2171-A2180. DOI: 10.1149/1.2352197
38. Zolfaghari A., Naderi H., Hamid R., Mortaheb R. Carbon black/manganese dioxide composites synthesized by sonochemistry method for electrochemical supercapacitors. *Journal of Electroanalytical Chemistry.* 2013, **Vol. 697,** p. 60–67. DOI:10.1016/j.jelechem.2013.03.012
39. Pang L.S., Saxby J.D., Chatfield S.P. Thermogravimetric Analysis of Carbon Nanotubes and Nanoparticles. *The Journal of Physical Chemistry.* 1993, **Vol. 97(27)**, p. 6941–6942. DOI: 10.1021/j100129a001
40. Liu X., Wen N., Wang X., Zheng Y. A High-Performance Hierarchical Graphene@Polyaniline@Graphene Sandwich Containing Hollow Structures for Supercapacitor Electrodes. *ACS Sustainable Chem. Eng*. 2015, **Vol. 3(3),** p. 475–482. DOI:10.1021/sc5006999